Revisiting velocity, concentration and interface measurements in a magnetic micromixer

F. Gökhan Ergin[1], Guntars Kitenbergs[2*], Andrejs Cēbers[2]

[1] Dantec Dynamics, Skovlunde, Denmark

[2] University of Latvia, MMML lab, Riga, Latvia

[*] guntars.kitenbergs@lu.lv

Abstract

Mixing is an important process in microfluidics and subtantial flow field investigation efforts are spent to achieve high performance micromixers. In this work, we revisit a magnetic micromixer experiment reported by Ergin et al. (2013). It exploits a phenomenon called magnetic micro-convection, which appears on an interface of miscible magnetic and nonmagnetic fluids. We have a goal to improve both the accuracy and the resolution of measurements, where micro particle image velocimetry system is used. For that we address improvements in two different areas. First is an improvement of the experimental system. Introducing microfluidics chip and controllable syringe pumps enable a better control of interface formation. Second is the quality of concentration measurements. Using an absorption calibration step we show that the concentration estimation from Beer-Lambert law can significantly alter results and cause errors. This is crucial for precise image analysis steps that rely on concentration plots or values. Improvements lead to more precise measurements of velocities, concentrations and phase boundaries, enabling detailed studies of the physical phenomena or their applications.

1 Introduction

Microfluidics technologies and lab-on-a-chip devices are gradually approaching market, but mixing diffusion limited laminar flows remains an important challenge. A lot of effort has been put to investigate processes and systems that improve mixing. Use of magnetic materials is particularly attractive, as they can be actuated from distance Chen and Zhang (2017). Here we revisit a magnetic micromixer, which works due to a phenomenon called magnetic micro-convection Ergin et al. (2013); Kitenbergs et al. (2015a). Compared to other mixers, a lot of work has been done on explaining the phenomenon and formulating a theoretical model Kitenbergs et al. (2015b). In addition, it has been investigated also in other geometries, i.e. radial Li et al. (2018) and sessile droplet Lee et al. (2018). However, quantitative and detailed verification and comparison demands better characterization of mixing flows, where Particle image velocimetry (PIV) and complementary image processing techniques are particularly useful. In addition, this can be used as a model problem, which allows to improve multiple measurement techniques.

The magnetic micromixer works on an interface of miscible magnetic and nonmagnetic fluids in a thin layer. When magnetic field is applied, the magnetic micro-convection instability appears on the interface and a particular finger like pattern is formed. We have measured these microflows with a MicroPIV already before Ērglis et al. (2013), however experimental setup had limited control and precision. Initial measurements gave way to advancing and applying various processing techniques, including modal analysis Ergin et al. (2014) and adding preprocessing functions Ergin et al. (2015). These and other PIV techniques for microfluidics are summarized in a recent review Ergin et al. (2018). Here we focus on improving determination of concentration and looking how it changes results of PIV image processing methods.

2 Experimental system

Experiments were performed using an experimental setup (see Fig. 1) based on a MicroPIV system manufactured by Dantec Dynamics. MicroPIV system consists of HiPerformance microscope (based on Leica
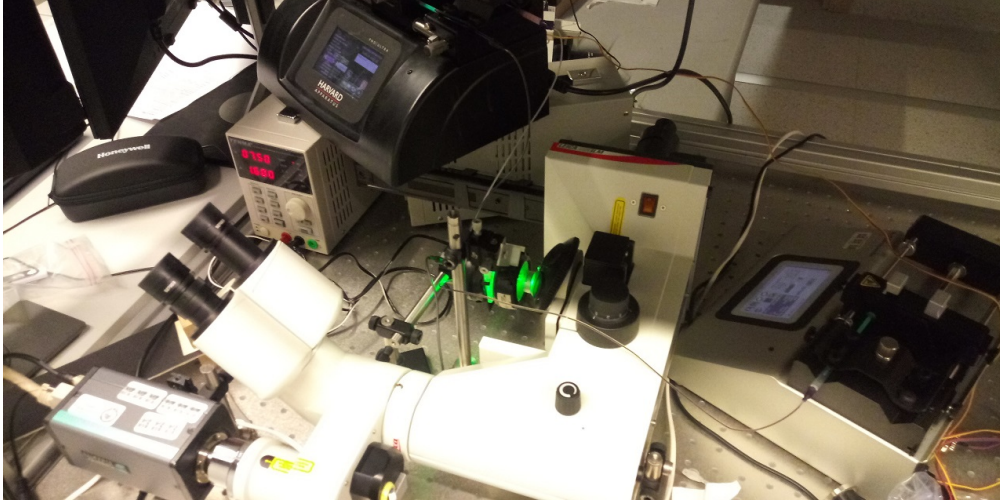
Figure 1: An image of the experimental setup, which is based on Dantec Dynamics MicroPIV system that is complemented by a magnetic coil and microfluidics system.

DMIL), double-frame camera HiSense MkII, LED microstrobe, timer box and a computer equipped with software DynamicStudio v6.2. It is complemented by a custom made magnetic coil that is powered by a power supply (TENMA) and can create homogeneous magnetic fields ranging from 0 to 10 mT. To enable microflows, a microfluidics chip, tubing and microfluidic syringe pumps (Harvard Apparatus, KD Scientific) are used. During magnetic micro-convection investigation, it was noticed that even the tiny channel thickness is sufficient for gravity induced convection Kitenbergs et al. (2018), where denser magnetic fluid wants to slide below the less dense water. To eliminate unwanted convection, we hold the sample vertically, placing denser magnetic fluid below the less dense water. Therefore also microscope and corresponding microPIV system is turned sideways.

For magnetic fluid we took maghemite nanoparticle colloid (made in PHENIX lab, Paris, France) with a volume fraction $\Phi = 2.8\%$, nanoparticle average diameter $d = 7.0$ nm, saturation magnetization $M_{sat} = 8.4$ G and magnetic susceptibility $\chi_m = 0.016$, as determined by a vibrating sample magnetometer (Lake Shore 7404). Miscible nonmagnetic fluid was deionized water. In order to visualize flows, we add $\Phi = 0.1\%$ plastic tracer particles with the average diameter $d = 1.0 \, \mu$m (Invitrogen).

Microfluidics chip is made in a simple and robust manner. We use a Parafilm®M spacer, in which channels are cut by a paper knife. Then this spacer is sandwiched between two microscope glass slides and heated on a hotplate until it makes a sealed chip. Syringe tips are glued in the drilled holes of the top glass slide and work as tubing connectors.

Fluids are introduced and extracted by two syringe pumps, which are synchronized by an Arduino control. This allows to start and stop flow in a highly controlled manner.

The experiments are done as follows. First, both fluids are introduced in chip with the same speed 50 μl/min, forming a sharp and moving interface. At the same time fluids are extracted from the outlet at a double speed 100 μl/min. Then the flows are stopped using synchronized control. Once interface stops, magnetic field is turned on. The process is filmed with the MicroPIV system, using 750 μs microstrobe double pulses at 6 Hz. The 0.7 x camera mount and the 10 x microscope objective produces a total system magnification 7 x. For camera this produces a 1.2×0.9 mm^2 field of view.

It is worth to mention that microsctrobe is placed on the other side of the microfluidics cell, providing bright field microscopy conditions. Hence, tracer particles provide contrast, but no fluorescent signal.

3 Image analysis and PIV

The acquired images are pre-processed following the same procedure as in Ergin et al. (2010). First a histogram inversion step is applied to have a bright signal for tracer particles. It is followed by Local contrast normalization (LCN) and Difference of Gaussion (DoG) filters.

PIV is done on the filtered images with the full field of view. The interrogation area (IA) is chosen so
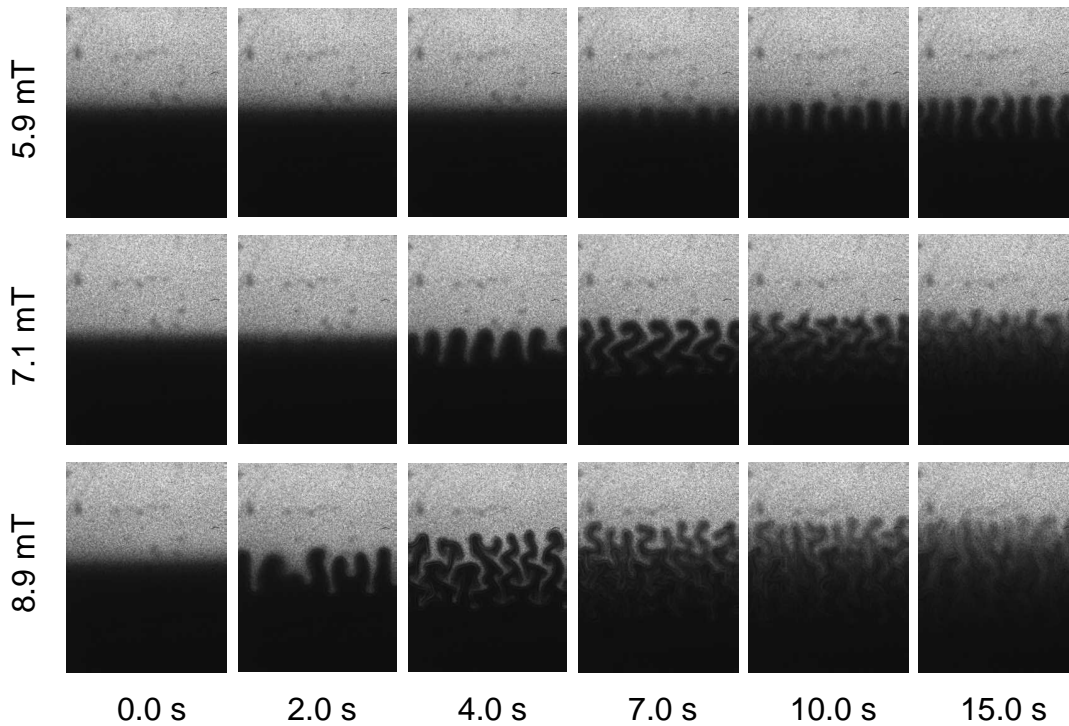
Figure 2: Image series of the magnetic micro-convection dynamics for three different field strengths. The field of view in each image is $1.2 \times 0.9 \text{mm}^2$ large.

that maximal IA size is 64×64 pixels, while minimal 32×32 pixels, while grid step size is 16 pixels in both directions. Validation is based on the peak height ratio, using 1.15. The flow field is corrected using the Universal outlier detection (UOD) in 5×5 neighborhood, where 0.1 is the minimum normalization, but 2 as the acceptance factor limit. In addition IA is adapted for particle density, while its shape is adapted to velocity gradients. From validated flow fields vorticities are calculated.

To find the phase boundary, we use Otsu threshold method Otsu (1979). We choose a concentration, with which we differentiate the two miscible phases, by saying that everything above this concentration is magnetic fluid phase, while below - water phase. In practice, we start with a global threshold, where an intensity region allows to roughly estimate the phase boundary location. The second step is application of local Otsu thresholding (LOT). It means that a local bounding box is extracted around each pixel of the boundary region in order to choose to which phase it belongs.

All image processing is done using DynamicStudio software.

4 Results and discussion

As known from previous research Kitenbergs et al. (2015b), characteristic dynamics of the magnetic micro-convection is field dependent. In Fig. 2 one can see the instability development for three different magnetic field values. Initially individual fingers form on the interface - magnetic fluid fingers towards water and water fingers towards magnetic fluid. Fingers growth continues until they start to bend and/or secondary fingers develop. Eventually, concentration smearing reaches a point where magnetic forces are insufficient to induce additional flow and magnetic nanoparticle diffusion takes over, slowly equalizing the concentrations.

As compared to previous magnetic micro-convection PIV measurements Ergin et al. (2013); Ērglis et al. (2013), the experiment quality and quality of images in particular has increased substantially. The interface is straight and the finger formation is clearly visible. Nevertheless, an additional improvement to the experiment is done. Until now we have assumed that the image intensity can provide us with the concentration information, assuming it follows the Beer-Lambert law. If we know the intensities of water and initial magnetic fluid (and we know them at least from the beginning of the experiment, when nothing has mixed), we
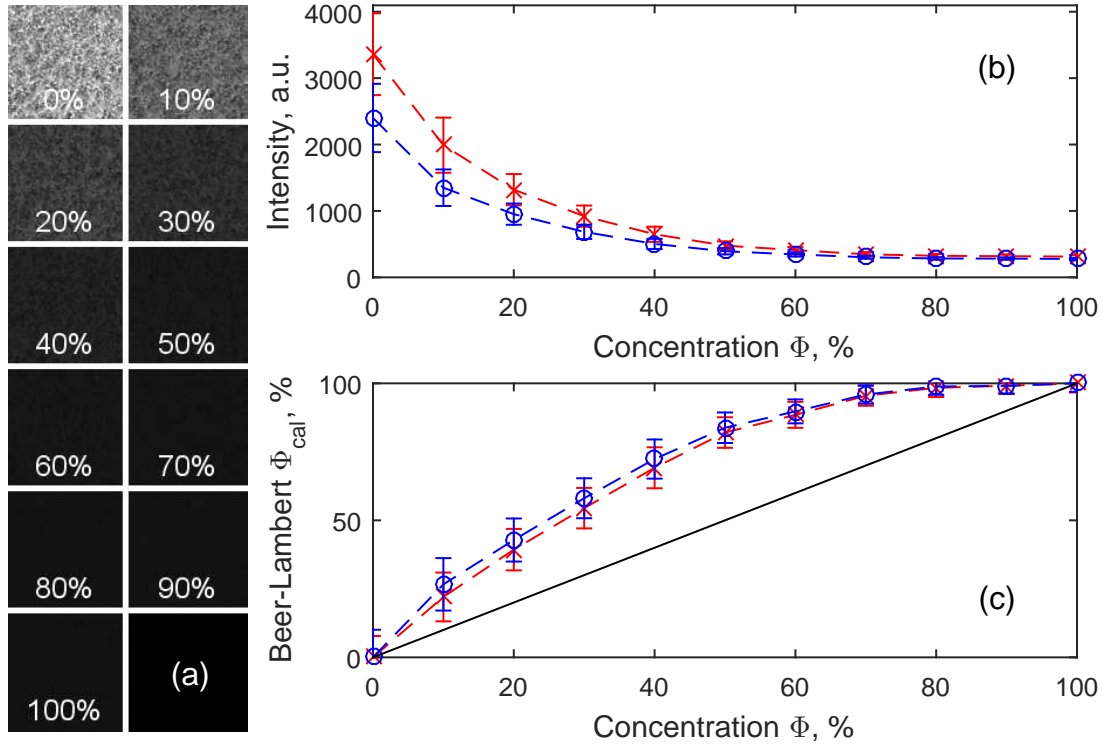
Figure 3: Magnetic fluid concentration calibration. (a) sample images for various magnetic fluid concentrations. (b) Average intensity dependence on magnetic fluid concentration for two different microstrobe pulse lengths. (c) Comparison between real magnetic fluid concentrations and values expected from Beer-Lambert law. In (b) and (c) Red crosses correspond to $t_p = 750\,\mu s$, while blue circles to $t_p = 500\,\mu s$. Black line in (c) marks positions where Beer-Labert and actual concentrations would agree.

can express the concentration as a function of intensities

$$\Phi_{cal}(x,y) = \frac{\log_{10} I(x,y) - \log_{10} I_{H_2O}}{\log_{10} I_{MF} - \log_{10} I_{H2O}}, \tag{1}$$

where $I(x,y)$ is the light intensity in point (x,y), I_{H_2O} is the average intensity of water and I_{MF} is the average intensity of original magnetic fluid. This displays a logarithmic relation that also includes 2 constants, which we can measure. We try to verify this with a calibration.

For calibration we prepare 11 samples with different concentrations of original magnetic fluid with tracer particles, by mixing it with water with tracer particles, so that we obtain magnetic fluid concentrations 0%, 10%, .. 100%. Each of the samples is imaged using the same system and settings as experimental images of the magnetic micro-convection. Sample images (0.25×0.25 mm^2 field of view) can be seen in Fig. 3 (a). One can easily see that the magnetic fluid concentrations above 50% are already quite dark.

To measure this quantitatively, we find the average intensity and its error (standard deviation) for each image with a different concentration. We do this for 2 different Microstrobe pulse lengths. As a result, we find an intensity decrease with an increase of magnetic fluid concentration that should be expected (Fig. 3 (b)).

We continue by calculating the Beer-Lambert concentration Φ_{cal} for each of the samples using Eq. 1. Fig. 3 (c) displays the relation between Beer-Lambert and actual concentration. A good agreement would be if the data point stayed on the black straight line. However, we can see that the Beer-Lambert concentrations are much larger than the actual ones. It means that we overestimate the concentration. Hence, in this case the use of Labert-Beer law is not valid. Instead, conversion of intensity images to concentration plots must be done using calibration data.

An illustration of what difference use of calibration data do, one can see Fig 4. (a) is a sample image. (b) shows the concentration plot if the concentrations are calculated using Eq. 1. One can see that in the water
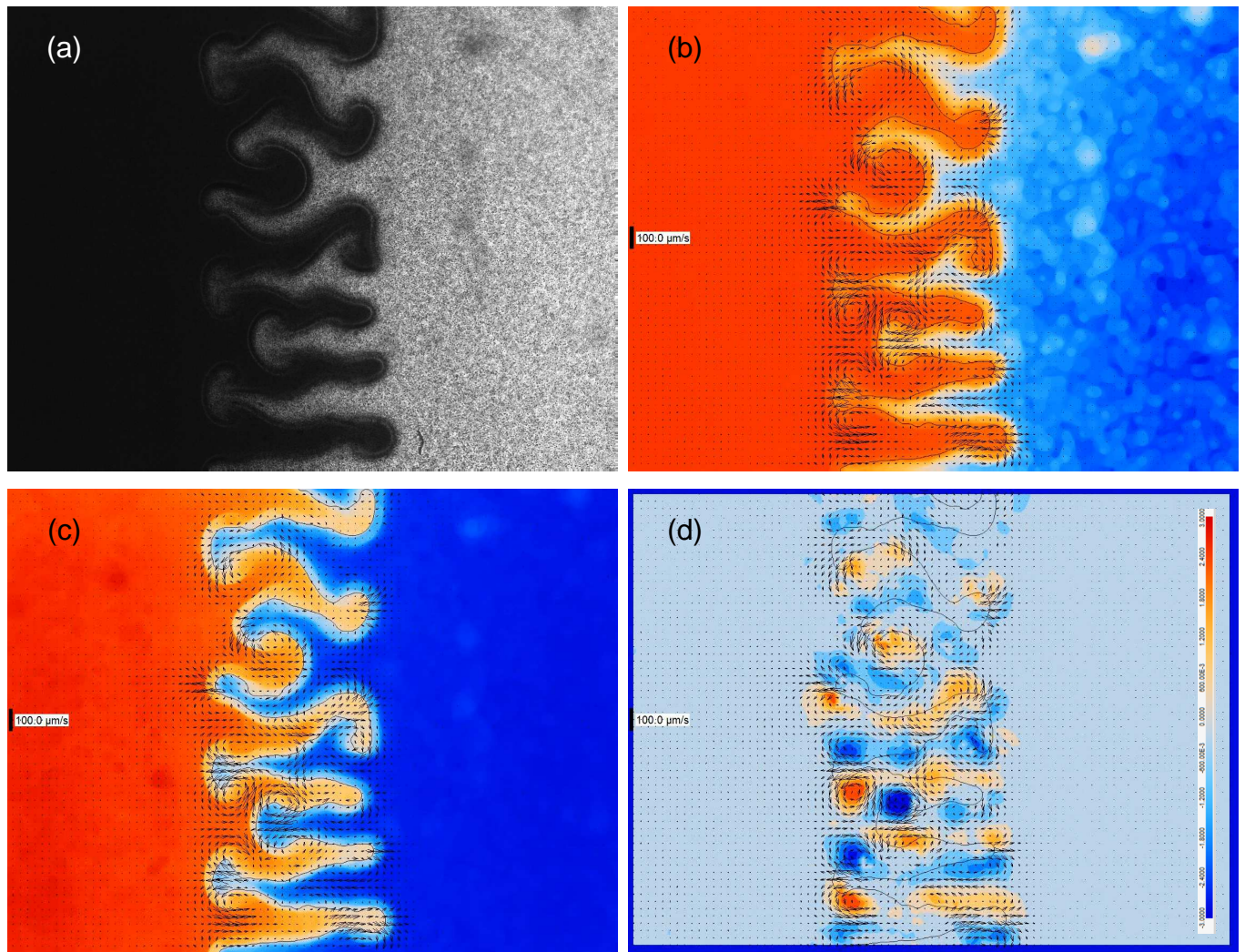
Figure 4: An example of image processing results. (a) Original snapshot of the magnetic micro-convection. (b) Beer-Lambert concentration plot. (c) Concentration plot using calibration. (d) Vorticity plot. All three (b), (c) and (d) show also phase boundary and flow field.

part a notable concentration distribution, which one would not expect. (c) displays the concentration plot using calibration data. It is clearly visible that concentration distributions in water part are much smaller. Concentration color scheme has red for original magnetic fluid, blue for water (no magnetic fluid) and white in the middle (50%). One can see that (c) looks much more symmetric than (b), as one expects in theoretical models and numerical simulations Kitenbergs et al. (2015b).

In addition to concentration plots, tracer particles allow us to find flow fields using PIV methods described before, while using the previously described Otsu threshold one can find the phase boundary. Both phase boundary and flow fields are shown on top of Fig 4 (b), (c) and (d). With a phase boundary we understand an area where a fixed magnetic fluid concentration is present, in our case it is 50% and characterizes the actual division of two miscible phases. This enables to proceed with different phase analysis methods. In (c) the quality of the phase boundary can be seen the best. It precisely follows the fingering pattern shape. While flow fields show that largest velocities are at the finger tips, indicating the growth process. Mushroom like finger tips show quick changes in the velocity vector directions. This is best seen in Fig 4 (d), where vorticity plot is displayed. Notable vortices of opposite signs are visible next to every mushroom like finger tip. Although, the magnification is only 7 x, one can already see very nice patterns and how velocity relates to the change in the pattern. It is planned to continue this by studying individual finger dynamics in a greater detail.
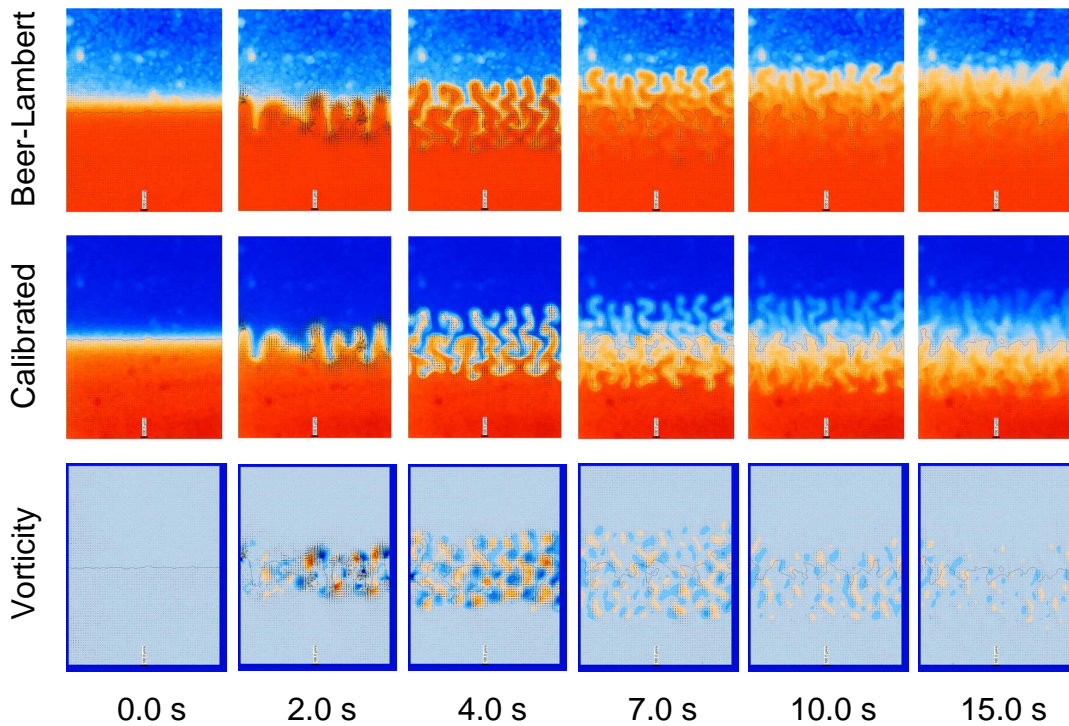
Figure 5: Magnetic micro-convection dynamics for $B = 8.9$ mT in Fig. 2 is visualized by the image processing results. First row corresponds to Beer-Lambert concentration plots, phase boundary and flow fields. Second - concentration plots that use calibration, phase boundary and flow fields. Third - vorticity data, phase boundary and flow fields.

To get a better impression on how the improved experimental system and concentration calibration improves the results, Fig. 5 displays Beer-Lambert concentration plots, calibrated concentration plots, vorticity plots as well as flow fields and phase boundary for the third row of images in Fig. 2, which corresponds to $B = 8.9$ mT and the same times.

Comparing both types of concentration plots, one can notice that calibration has corrected the concentration distribution and the magnetic micro-convection dynamics looks much more symmetric. Also vorticity dynamics displays the few strong vortices in the beginning, many less strong vortices in the middle and a few vortices further away from the phase boundary, indicating the decay of the convective motion. Both of these things qualitatively agree very well with numerical simulations, but a more detailed comparison is necessary, for example, with Kitenbergs et al. (2015b).

From figures we can see that using calibration gives a good concentration plot estimate, which can be further used in pattern analysis, etc. The calibration itself shows a large difference from the results using Beer-Lambert law, which means that either concentrations are too large for the law to be used, camera settings have some specific nonlinear sensitivity configuration or any other reason. Nevertheless, we have to recognize that in multiple of our previous articles the Beer-Lambert law approximation was inaccurate and should not have been used. For example in Ergin et al. (2013); Kitenbergs et al. (2015b). Now we will know how to approach it appropriately. Moreover, as the characteristic parameters (concentration, sample thickness, timescale) of this experiment, as well as the camera are rather typical, then the need for a calibration step should be considered, whenever a concentration plot is needed from an image.

5   Conclusion

We have revisited a magnetic micromixer. It mixes magnetic and nonmagnetic fluids in magnetic micro-convection process and provides a useful playground for PIV technique development. The improvement in experimental setup, calibration procedure and interface detection improves the results significantly com-

pared to Ergin et al. (2013)

Rotation of the experimental system by 90 degrees eliminated the magnetic fluid slip under water, which allowed to study microflows in a more true 2D environment. In addition, the advanced fluid control allows to form a flat interface. These improvements make the experiment much closer to theoretical model and simulations Kitenbergs et al. (2015b) and allow a better comparison between them.

Until now we trusted the assumption that light absorption changes linearly with concentration (Beer-Lambert law), but here we prove that it does not work for our conditions, which are rather typical. Therefore we have included a concentration calibration step. This results in an accurate concentration plot, which is both useful for comparison with numerical simulations and further image analysis. For example, here it allows to better identify the phase boundary (where concentration is at 50%). This is an improvement compared to previous analysis Ergin et al. (2013), because of using calibration information, global thresholding and local Otsu thresholding. Also the fingers of the instability can be seen on both sides of the original interface, which was not the case previously.

These results let us be confident about interface location, therefore future work will focus on phase separated PIV measurements, which will further improve the flow field accuracy along the interface. As a result, one has not only possibilities to better study fundamental understanding of the magnetic micro-convection, but also enable other unique and innovative measurements in microfluidics.

Acknowledgements

References

Chen X and Zhang L (2017) A review on micromixers actuated with magnetic nanomaterials. *Microchimica Acta* 184:3639–3649

Ergin FG, Watz B, and Gade-Nielsen N (2018) A review of planar piv systems and image processing tools for lab-on-chip microfluidics. *Sensors* 18:3090

Ergin FG, Watz BB, Ērglis K, and Cēbers A (2010) Poor-Contrast Particle Image Processing in Microscale Mixing. in *ASME 2010 10th Biennial Conference on Engineering Systems Design and Analysis - Istambul, Turkey, Jul 12-14*

Ergin FG, Watz BB, Ērglis K, and Cēbers A (2013) Planar velocity and concentration measurements in a magnetic micromixer with interface front detection. in *10th International Symposium on Particle Image Velocimetry - PIV13, Delft, The Netherlands, July 1-3*

Ergin FG, Watz BB, Ērglis K, and Cēbers A (2014) Modal analysis of magnetic microconvection. *Magnetohydrodynamics* 50:339–352

Ergin FG, Watz BB, Ērglis K, and Cēbers A (2015) Time-resolved velocity measurements in a magnetic micromixer. *Experimental Thermal and Fluid Science* 67:6 – 13. heat Transfer and Fluid Flow in Microscale

Ērglis K, Tatulcenkov A, Kitenbergs G, Petrichenko O, Ergin FG, Watz BB, and Cēbers A (2013) Magnetic field driven micro-convection in the hele-shaw cell. *Journal of Fluid Mechanics* 714:612–633

Kitenbergs G, Ērglis K, Perzynski R, and Cēbers A (2015a) Magnetic particle mixing with magnetic micro-convection for microfluidics. *Journal of Magnetism and Magnetic Materials* 380:227 – 230

Kitenbergs G, Tatulcenkovs A, Ērglis K, Petrichenko O, Perzynski R, and Cēbers A (2015b) Magnetic field driven micro-convection in the hele-shaw cell: the brinkman model and its comparison with experiment. *Journal of Fluid Mechanics* 774:170–191

Kitenbergs G, Tatulcenkovs A, Pukina L, and Cēbers A (2018) Gravity effects on mixing with magnetic micro-convection in microfluidics. *Eur Phys J E* 41:138

Lee JG, Porter V, Shelton WA, and Bharti B (2018) Magnetic field-driven convection for directed surface patterning of colloids. *Langmuir* 34:15416–15424

Li H, Kao CY, and Wen CY (2018) Labyrinthine and secondary wave instabilities of a miscible magnetic fluid drop in a hele-shaw cell. *Journal of Fluid Mechanics* 836:374–396

Otsu N (1979) A threshold selection method from gray-level histograms. *IEEE Transactions on Systems, Man, and Cybernetics* 9:62–66